Binding Modes in Peptides

DOI: 10.1002/anie.201410389

Multi-Frequency, Multi-Technique Pulsed EPR Investigation of the Copper Binding Site of Murine Amyloid β Peptide**

*Donghun Kim, Jeong Kyu Bang, and Sun Hee Kim**

Abstract: *Copper-amyloid peptides are proposed to be the cause of Alzheimer's disease, presumably by oxidative stress. However, mice do not produce amyloid plaques and thus do not suffer from Alzheimer's disease. Although much effort has been focused on the structural characterization of the copper-human amyloid peptides, little is known regarding the copper-binding mode in murine amyloid peptides. Thus, we investigated the structure of copper-murine amyloid peptides through multi-frequency, multi-technique pulsed EPR spectroscopy in conjunction with specific isotope labeling. Based on our pulsed EPR results, we found that Ala2, Glu3, His6, and His14 are directly coordinated with the copper ion in murine amyloid β peptides at pH 8.5. This is the first detailed structural characterization of the copper-binding mode in murine amyloid β peptides. This work may advance the knowledge required for developing inhibitors of Alzheimer's disease.*

Alzheimer's disease (AD) is a well-known neurodegenerative disease that has received considerable attention as the population of patients suffering from this disease grows rapidly.[1] The most common pathological feature of AD is the extracellular deposits of amyloid β peptide (Aβ) plaques, and interestingly, the concentration of metal ions such as copper in the plaques is high.[2] This finding leads to the hypothesis of metal-induced amyloid fibrilization by oxidative stress owing to the reaction between redox-active metal ions and oxygen.[3] Because a detailed knowledge of the coordination environment of copper is required to understand the molecular mechanism of the amyloid fibrilization event, extensive efforts have been focused on elucidating the coordination of copper ions in human amyloid β peptides (hAβ).[4,5]

Murine amyloid β peptides (mAβ), however, differ from hAβ in three amino acids: R5G, Y10F, and H13R. It has been shown that these three different amino acid residues make mAβ soluble, without peptide fibrilization, and thus, Aβ deposition is not encountered in rats.[6] Furthermore, copper has long been known to ligate to the mAβ, and the coordination of Cu^{II} in mAβ has been proposed to be different from that in hAβ.[7,8] However, the detailed structure of Cu^{II}-mAβ has not been thoroughly studied.[8,9] To better understand the AD mechanism, investigations involving mouse animal models are essential. Therefore, it is of particular importance to elucidate the structure of the copper-coordinated murine amyloid peptide (Cu-mAβ), which may provide insight into the aggregation mechanism of amyloid peptides.

In this work, we employed multi-frequency, multi-technique pulsed electron paramagnetic resonance (EPR) spectroscopy to explore the details of the copper coordination of mAβ. A combination of 9 GHz hyperfine sublevel correlation (HYSCORE) and 34 GHz electron nuclear double resonance (ENDOR) spectroscopy along with specific isotope labeling is immensely useful for identifying the coordination environment of the copper binding site in mAβ. A set of specifically isotope-labeled mAβ peptides consisting of uniformly ^{13}C- and ^{15}N-labeled Ala2, ^{13}C-and ^{15}N-labeled Glu3, ^{15}N-labeled His6, and ^{15}N-labeled His14 was used.

The CW-EPR of Cu-mAβ at pH 7.4 exhibits two distinct sets of hyperfine peaks of the copper ion. This EPR spectrum can be effectively reproduced in simulations involving two different copper species (Supporting Information, Figure S1). As the pH was raised to 8.5, the CW-EPR of Cu-mAβ showed only one species, which is comparable to the results observed for Cu-mAβ.[9] The spectrum at pH 8.5 can be well simulated using $g = [2.23, 2.06, 2.06]$ and $A = [154, 14, 14]$ G (Supporting Information, Figure S1). Thus, owing to the complexity of the interpretation, we will exclusively focus on examining the coordination environment of the Cu-mAβ at pH 8.5. Furthermore, no effect of isotope labeling on the EPR spectra was observed (Supporting Information, Figure S2). Thus, high-resolution pulsed EPR techniques were used to detect hyperfine interactions not observed in the CW-EPR.

To probe the detailed coordination environment of the copper site in mAβ, 9 GHz HYSCORE experiments were conducted. A two-dimensional HYSCORE spectrum consists of cross-peaks that represent correlations between the nuclear frequencies of one electron spin manifold and the nuclear frequencies of the other electron spin manifold, simplifying the analysis of spectra.[10] Figure 1a displays the HYSCORE spectrum of natural-abundance Cu-mAβ, which shows the cross-peaks near (4.0, 1.6) and (1.6, 4.0) MHz. These peaks have been assigned as the double-quantum of the amino nitrogen nucleus of histidine (His) directly bound to

[*] D. Kim, Dr. S. H. Kim
Western Seoul Center, Korea Basic Science Institute
Seoul 120-140 (Korea)
E-mail: shkim7@kbsi.re.kr
Dr. J. K. Bang
Division of Magnetic Resonance Korea Basic Science Institute, Ochang
Chungbuk 363-883 (Korea)

[**] This work was supported by KBSI grant (T34435) to S.H.K. We gratefully appreciate Prof. Brian M. Hoffman and Dr. Peter Doan at Northwestern University for providing the ENDOR simulation code and Dr. Kyung-Bin Cho at Ewha Womans University for his help with DFT calculations.

Supporting information for this article is available on the WWW under http://dx.doi.org/10.1002/anie.201410389.

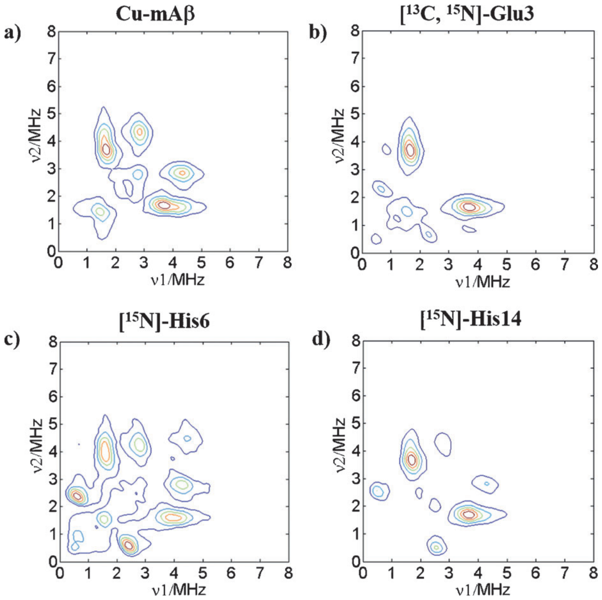

Figure 1. HYSCORE spectra of a) Cu^{II}-mAβ(1–16), b) ^{13}C,^{15}N-Glu3-Cu^{II}-mAβ(1–16), c) ^{15}N-His6-Cu^{II}-mAβ(1–16), and d) ^{15}N-His14-Cu^{II}-mAβ(1–16). Experimental conditions: microwave frequency 9.7 GHz, magnetic field 3360 G, $T=12$ K, π pulse width 32 ns, π/2 pulse width 16 ns, $\tau=210$ ns (except in (a): $\tau=140$ ns).

Cu^{II}.[11,12] This assignment can be verified using isotope-labeled histidines.

When the HYSCORE experiments were performed on ^{15}N-labeled His6 peptides, along with the features present in the unlabeled peptide, new cross-peaks at about (2.4, 0.6) and (0.6, 2.4) MHz centered at the Larmor frequency of ^{15}N ($\nu_{15N}=1.45$ MHz) and split by 1.8 MHz appeared (Figure 1c). These cross-peaks arise from the correlation between the ^{15}N transitions in different electron spin manifolds. These weakly coupled nitrogen atoms are characteristic of the amino nitrogen of a histidine directly bound to the copper ion.[10,13] Furthermore, the HYSCORE spectra taken with ^{15}N-labeled His14 peptides are similar to the spectra of ^{15}N-labeled His6, which indicates that the hyperfine parameters are nearly identical. Thus, HYSCORE experiments in conjunction with the ^{15}N isotope labeling of histidines indicate that both His6 and His14 bind directly to the copper ion (Figure 1c,d).

The HYSCORE spectrum of natural-abundance Cu^{II}-mAβ shows another set of cross-peaks at (4.4, 2.9) and (2.9, 4.4) MHz (Figure 1a). To identify these cross-peaks, additional HYSCORE experiments were conducted on the ^{15}N-labeled Glu3 of mAβ. In the HYSCORE of the ^{15}N-labeled Glu3 sample, these cross-peaks disappear, which is unambiguously confirmed by the appearance of the ^{15}N signal in the HYSCORE (Figure 1b). The cross-peaks near (2.3, 0.7), (0.7, 2.3) MHz centered at the ^{15}N Larmor frequency ($\nu_{15N}=1.45$ MHz) with a splitting of approximately 1.6 MHz are clearly shown in the HYSCORE of ^{15}N-labeled Glu3 of Cu^{II}-mAβ. Thus, the HYSCORE experiments show that the cross-peaks at (4.4, 2.9) and (2.9, 4.4) MHz in Cu-mAβ arise from the ^{14}N of Glu3. Furthermore, the shape and the position of this feature are strikingly comparable to observations for the double-quantum transitions of an amide nitrogen atom of a non-coordinating peptide backbone when the adjacent carbonyl function is coordinated with the Cu^{II} ion in the equatorial position.[5,11,14] This assignment can be further verified by the pulsed EPR data taken on the ^{13}C-labeled Ala2 samples (see below).

The HYSCORE experiments on the ^{13}C-labeled Ala2 of Cu^{II}-mAβ exhibit strong ^{13}C ridges centered on the ^{13}C Larmor frequency ($\nu_{13C}=3.6$ MHz). At $g_{\perp}$, the ^{13}C ridges of Ala2 exhibit a splitting of approximately 2.4 MHz and a width of approximately 0.9 MHz with a larger splitting of approximately 3.4 MHz in the $g_{\parallel}$ region (Figure 2).

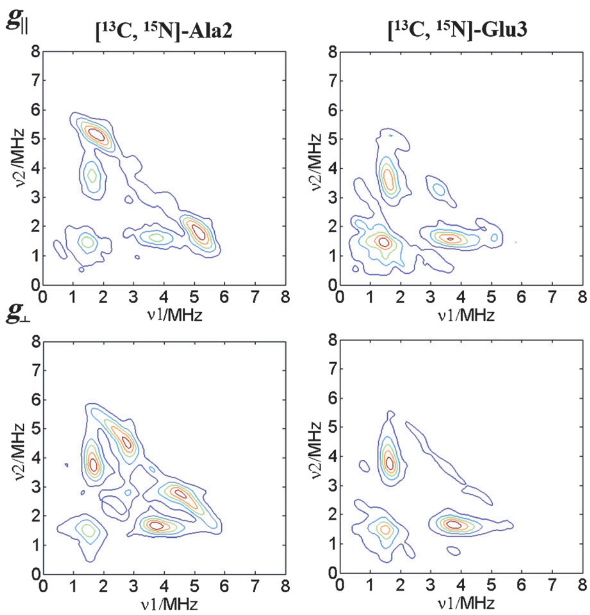

Figure 2. HYSCORE spectra of ^{13}C,^{15}N-Ala2 Cu^{II}-mAβ(1–16) (left), and ^{13}C,^{15}N-Glu3-Cu^{II}-mAβ(1–16) (right) at $g_{\parallel}$ (top) and $g_{\perp}$ (bottom). Experimental conditions: microwave frequency 9.7 GHz, $T=12$ K, π pulse width 32 ns, π/2 pulse width 16 ns, $\tau=140$ ns.

This ^{13}C signal was confirmed by Mims ENDOR. Figure 3 shows the ^{13}C Mims ENDOR of globally labeled ^{13}C of Ala2 Cu-mAβ taken across the EPR envelope. The ENDOR features are centered on the ^{13}C Larmor frequency and split by the magnitude of hyperfine interactions. The ^{13}C ENDOR shows doublets centered at the Larmor frequency of ^{13}C and separated by 4.4 MHz around $g_{\parallel}$, decreasing to 2.4 MHz as the field changes to $g_{\perp}$. The τ value of 150 ns was chosen to prevent the suppression effect of Mims holes at $A=n/\tau$ ($n=0,1,2,\ldots$).[15] By collecting the ^{13}C Mims ENDOR throughout the EPR envelop of Cu-mAβ, we were able to extract the ^{13}C hyperfine tensor parameters to more accurately map the location of the ^{13}C nucleus of Ala2.

The 2D field-frequency ENDOR signals are well simulated by $A=[1.8, 3.0, 4.6]$ MHz and Euler angles $[\beta, \alpha]=[80, 10]°$. The magnitude of the hyperfine coupling (A_{iso}) of ^{13}C approximately 3 MHz can be explained by a through-bond pathway resulting from the equatorial coordination of the carbonyl oxygen of Ala2 with a Cu^{II} ion.[16] Additionally, the Cu^{II}–^{13}C vector in the g frame with the Euler angles obtained from the simulations indicates that the ^{13}C nucleus is located

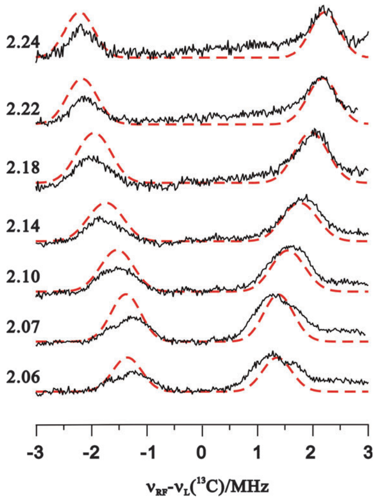

Figure 3. 2D field/frequency ^{13}C Mims ENDOR spectra of globally labeled ^{13}C,^{15}N-Ala2 Cu^{II}-mAβ(1–16). Experimental conditions: microwave frequency 33.8 GHz, $T=12$ K, Mims ENDOR $\pi/2$ width 32 ns, $\tau=150$ ns, RF pulse width 20 μs. Simulations are shown with red dashed lines: simulation parameters: $g=[2.23, 2.06, 2.06]$, $A=[1.8, 3.0, 4.6]$ MHz, Euler angles $=[\beta, \alpha]=[80, 10]$°.

near the equatorial position. Thus, the ^{13}C-labeled Ala2 HYSCORE and the Mims ENDOR spectroscopy together with the ^{15}N HYSCORE of Glu3 demonstrate that the carbonyl of Ala2 is an equatorial ligand of the copper ion.

Another ^{13}C ENDOR signal with very weak hyperfine coupling of approximately 0.5 MHz was detected when using different τ values to maximize the sensitivity of the smaller hyperfine couplings because the ENDOR response R depends on the hyperfine coupling A and the time τ between the first two $\pi/2$ pulses according to the equation $R \approx [1-\cos(2\pi A\tau)]$ (Supporting Information, Figure S3).[15] This smaller ENDOR signal may arise from the distant ^{13}C nucleus from the globally labeled ^{13}C of Ala2.

Interestingly, when a different τ value of 140 ns was used for the HYSCORE of the ^{13}C,^{15}N-labeled Glu3 of Cu-mAβ peptides, new ridges centered on the ^{13}C Larmor frequency ($\nu_{13C} \approx 3.6$ MHz) appeared, as shown in Figure 2. No features of the ^{13}C from Glu3 were detected in hAβ. The contour plot obtained near $g_{\parallel}$ displays more distinct ^{13}C cross-peaks at (5.1, 1.5), (1.5, 5.1) MHz with a splitting of approximately 3.6 MHz and another weakly coupled ^{13}C signal near the ^{13}C Larmor frequency. At $g_{\perp}$, there are two distinct ^{13}C signals: one is split by approximately 2 MHz with a width of approximately 0.5 MHz and the other is near the ^{13}C Larmor frequency with a ridge of approximately 1 MHz. Moreover, the ^{13}C signals of Glu3 are confirmed by the Mims ENDOR. The ^{13}C Mims ENDOR using different τ values is shown in the Supporting Information, Figure S4. The spectra were obtained near $g_{\perp}$, where the EPR intensity is maximized. To verify more or less broad and featureless ENDOR signals, different τ values were used. Using different τ values, the Mims holes due to the suppression effect (see below) appeared in the approximately 3 MHz ENDOR signal. This effect on the spectrum clearly indicates a strongly coupled ^{13}C hyperfine coupling of approximately 3 MHz.

Two more weakly coupled ^{13}C signals split by less than 1 MHz were also detected, with τ values of 300 ns and 500 ns (Supporting Information, Figure S4), which may arise from an axially coordinated or non-coordinated carboxylate ^{13}C of the side chains of Glu3 (see below). Although the ENDOR intensity is not strong enough to be detected throughout the EPR envelope, the magnitude of the hyperfine coupling (approximately 3 MHz) of the ^{13}C implies that the carbonyl or carboxyl of Glu3 is directly ligated to the copper ion,[16] suggesting two possible binding modes of Glu3 to the copper ion. One possibility is that this signal can be attributed to the ^{13}C of the carboxyl of an equatorially coordinated carboxylate directly coordinated with the copper site. The other is that the ^{13}C signal arises from the spin density on the ^{13}C carbon owing to the oxygen coordination of its backbone carbonyl (Supporting Information, Figure S5).

To distinguish between these two possible models, DFT calculation was performed. The DFT calculation demonstrates that the model with the oxygen coordination from the carboxyl side-chain of Glu3 is more stable than the model with coordination from the carbonyl backbone. The DFT-optimized structure of Cu-mAβ based on the results of this work is shown in Figure 4. Both His6 and His14 are coordinated with the copper site, and both the oxygen of the carbonyl of Ala2 and the oxygen of the carboxyl of the side-chain in Glu3 are ligands of the copper ion.

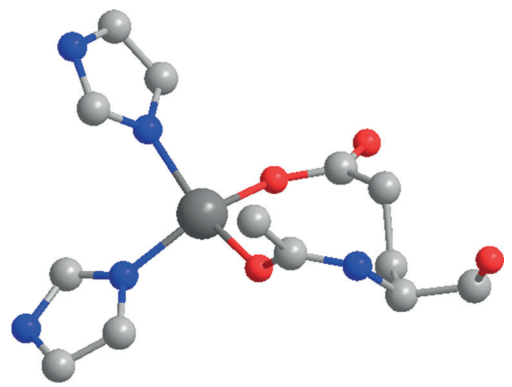

Figure 4. DFT-optimized structure of Cu^{II} binding site in mAβ based on our spectroscopic data. Ala2, Glu3, His6, and His14 are coordinated to the Cu^{II}. Cu dark gray, C gray, N blue, O red.

The coordination structure of the Cu-mAβ obtained from the spectroscopic and DFT calculations is similar to the proposed structure of the Cu-hAβ at high pH in that His6, His14, and Ala2 are coordinated with the copper ion.[4d] However, the coordination of Glu3 has not been observed in Cu-hAβ, which makes the binding mode of the Cu^{II} in rat Aβ unique. Although detailed mechanistic studies are required, the difference between humans and rats in the development of AD may lie in the nature of the Cu^{II} coordination by Glu3, which thus may have a key role in preventing amyloid fibrilization.

In summary, we have presented the detailed coordination environment of the copper-binding site in mAβ. By using multi-frequency, multi-technique pulsed EPR spectroscopy in conjunction with specific isotope labeling, we were able to directly detect and thus identify the ligands of the copper ion coordinated with murine amyloid peptides. This first detailed structural description of the copper-binding site in mAβ may help elucidate the molecular mechanism underlying amyloid fibrilization, providing structural insight into the development of inhibitors of Alzheimer's disease.

Received: October 23, 2014
Published online: December 10, 2014

Keywords: Alzheimer's disease · ENDOR · EPR spectroscopy · HYSCORE · murine amyloid peptides

[1] a) R. Jakob-Roetne, H. Jacobsen, *Angew. Chem. Int. Ed.* **2009**, *48*, 3030–3059; *Angew. Chem.* **2009**, *121*, 3074–3105; b) L. E. Scott, C. Orvig, *Chem. Rev.* **2009**, *109*, 4885–4910; c) E. Gaggelli, H. Kozlowski, D. Valensin, G. Valensin, *Chem. Rev.* **2006**, *106*, 1995–2044.
[2] D. J. Selkoe, *Physiol. Rev.* **2001**, *81*, 741–766.
[3] a) A. I. Bush, *Alzheimer Dis. Assoc. Disord.* **2003**, *17*, 147–150; b) A. Rauk, *Chem. Soc. Rev.* **2009**, *38*, 2698–2715; c) C. Hureau, P. Faller, *Biochimie* **2009**, *91*, 1212–1217; d) A. I. Bush, *Trends Neurosci.* **2003**, *26*, 207–214.
[4] a) S. C. Drew, K. J. Barnham, *Acc. Chem. Res.* **2011**, *44*, 1146–1155; b) B. K. Shin, S. Saxena, *Biochemistry* **2008**, *47*, 9117–9123; c) B. K. Shin, S. Saxena, *J. Phys. Chem. A* **2011**, *115*, 9590–9602; d) S. C. Drew, C. J. Noble, C. L. Masters, G. R. Hanson, K. J. Barnham, *J. Am. Chem. Soc.* **2009**, *131*, 8760–8761; e) J. W. Karr, L. J. Kaupp, V. A. Szalai, *J. Am. Chem. Soc.* **2004**, *126*, 13534–13538; f) J. W. Karr, V. A. Szalai, *J. Am. Chem. Soc.* **2007**, *129*, 3796–3797; g) P. Dorlet, S. Gambarelli, P. Faller, C. Hureau, *Angew. Chem. Int. Ed.* **2009**, *48*, 9273–9276; *Angew. Chem.* **2009**, *121*, 9437–9440; h) C. Hureau, Y. Coppel, P. Dorlet, P. L. Solari, S. Sayen, E. Guillon, L. Sabater, P. Faller, *Angew. Chem. Int. Ed.* **2009**, *48*, 9522–9525; *Angew. Chem.* **2009**, *121*, 9686–9689; i) D. Kim, N. H. Kim, S. H. Kim, *Angew. Chem. Int. Ed.* **2013**, *52*, 1139–1142; *Angew. Chem.* **2013**, *125*, 1177–1180.
[5] S. C. Drew, C. J. Noble, C. L. Masters, G. R. Hanson, K. J. Barnham, *J. Am. Chem. Soc.* **2009**, *131*, 1195–1207.
[6] a) C. Duyckaerts, M.-C. Potier, B. Delatour, *Acta Neuropathol.* **2008**, *115*, 5–38; b) O. Philipson, A. Lord, A. Gumucio, P. O'Callaghan, P. Lannfelt, L. N. Nilsson, *FEBS J.* **2010**, *277*, 1389–1409.
[7] T. Kowalik-Jankowska, M. Ruta, K. Wis'niewska, L. Łankiewicz, *J. Inorg. Biochem.* **2003**, 95, 270–282.
[8] E. Gaggelli, Z. Grzonka, H. Kozlowski, C. Migliorini, E. Molteni, D. Valensin, G. Velanlsin, *Chem. Commun.* **2008**, 341–343.
[9] H. Eury, C. Bijani, P. Faller, C. Hureau, *Angew. Chem. Int. Ed.* **2011**, *50*, 901–905; *Angew. Chem.* **2011**, *123*, 931–935.
[10] P. Höfer, A. Grupp, H. Nebenführ, M. Mehring, *Chem. Phys. Lett.* **1986**, *132*, 279–282.
[11] C. S. Burns, E. Aronoff-Spencer, C. M. Dunham, P. Lario, N. I. Avedievich, W. E. Antholine, M. M. Olmstead, A. Vrielink, G. J. Gerfen, J. Peisach, W. G. Scott, G. L. Millhauser, *Biochemistry* **2002**, *41*, 3991–4001.
[12] F. Jiang, J. McCracken, J. Peisach, *J. Am. Chem. Soc.* **1990**, *112*, 9035–9044.
[13] A. Lai, H. L. Flanagan, D. J. Singel, *J. Chem. Phys.* **1988**, *89*, 7161–7166.
[14] Y. Deligiannakis, M. Louloudi, N. Hadjiliadis, *Coord. Chem. Rev.* **2000**, *204*, 1–112.
[15] A. Schweiger, G. Jeschke, *Principles of Pulsed Electron Paramagnetic Resonance*, Oxford University Press, Oxford, **2001**.
[16] a) P. M. Schosseler, B. Wehrli, A. Schweiger, *Inorg. Chem.* **1997**, *36*, 4490–4499; b) D. Baute, D. Arieli, F. Neese, H. Zimmermann, B. M. Weckhuysen, D. Goldfarb, *J. Am. Chem. Soc.* **2004**, *126*, 11733–11745.

